



Taylor wavelet method for fractional delay differential equations

Phan Thanh Toan¹ · Thieu N. Vo¹ · Mohsen Razzaghi² 

Received: 19 December 2018 / Accepted: 1 July 2019 / Published online: 15 July 2019
© Springer-Verlag London Ltd., part of Springer Nature 2019

Abstract

We present a new numerical method for solving fractional delay differential equations. The method is based on Taylor wavelets. We establish an exact formula to determine the Riemann–Liouville fractional integral of the Taylor wavelets. The exact formula is then applied to reduce the problem of solving a fractional delay differential equation to the problem of solving a system of algebraic equations. Several numerical examples are presented to show the applicability and the effectiveness of this method.

Keywords Taylor wavelet · Delay differential equation · Numerical solution · Fractional integral · Collocation method

1 Introduction

Fractional differential equations (FDEs) have a long history. It can be traced back to the works of L'Hopital since 1695 when he raised a question to Leibniz about derivative of order $\frac{1}{2}$. In the last two decades, FDEs have drawn increasing attention due to their important applications in various fields of mathematics, sciences and engineering, such as electrochemistry [1], economic [2], mechanic [3, 4], medicine [5], signal processing [6], traffic model [7], and informatics [8].

Delay differential equation is a special kind of differential equation in which the derivative of the unknown function at a certain time is given in terms of not only the value of the unknown function at the same time, but also the values of the unknown function at previous times. Delay differential equations are introduced during various mathematical modelling of processes in engineering and sciences, such as economy, biology, medicine, chemistry, control, and electrodynamic

(see for instance, [9, 10] and references therein). In general, the solution of some delay differential equations cannot be expressed in terms of elementary functions. Therefore, it is necessary to develop numerical methods to approximate the solution of these equations. Variety of numerical solution methods have been proposed, for instance, Adomian decomposition method [11], One-leg θ -method [12], variational method [13], Legendre wavelet method [14], Chebyshev polynomials [15], and Bernoulli operational matrices [16].

Fractional delay differential equation is a natural generalization of delay differential equations of integer orders. However, there were not many works devoted to numerical methods for solving such kinds of differential equations. Some available numerical methods for solving fractional delay differential equations are based on finite difference method [17], Legendre pseudo-spectral functions [18], spectral collocation method [19], Hermit wavelet functions [20], Bernoulli wavelet functions [21], and linear interpolation method [22].

In recent years, wavelet theory has received considerable attention because of its powerful applications in several fields such as system analysis, numerical analysis, and optimal control [23]. Wavelets have several specific properties that make them useful [24]. In general, for solving fractional calculus using wavelets, the following equation has been used:

$$I^\alpha \Psi(t) \approx P^\alpha \Psi(t),$$

where I^α is the Riemann–Liouville fractional integral of order α for different wavelets and P^α the operational matrix for Riemann–Liouville integration (OMRLI). The elements

✉ Mohsen Razzaghi
razzaghi@math.msstate.edu

Phan Thanh Toan
phanthanhtoan@tdtu.edu.vn

Thieu N. Vo
vongochthieu@tdtu.edu.vn

¹ Fractional Calculus, Optimization and Algebra Research Group, Faculty of Mathematics and Statistics, Ton Duc Thang University, Ho Chi Minh City, Vietnam

² Department of Mathematics and Statistics, Mississippi State University, Starkville, USA

of $\Psi(t)$ are the basis functions. Typical examples are the applications of Chebyshev, Legendre, Cosine and Sine (CAS), or Haar wavelets [25–28]. For obtaining P^α , these wavelets were first expanded into block-pulse functions, then the OMRLI of block-pulse functions was used for calculating P^α . In addition, for obtaining P^α , using Bernoulli wavelets in [29], the Bernoulli wavelets were first expanded into Bernoulli polynomials, then the OMRLI of Bernoulli polynomials was used for calculating P^α for Bernoulli wavelets. It is noted that none of these wavelets calculated P^α directly, and some approximations were involved for calculating $I^\alpha\Psi(t)$.

A fractional delay differential equation can be stated as follows:

$$\begin{cases} D^\alpha y(x) = f(x, y(x), y(x - \tau)), & x \in [0, 1], \alpha > 0, \tau \in (0, 1), \\ y^{(i)}(0) = \lambda_i, & i = 0, \dots, [\alpha], \\ y(x) = \phi(x), & x < 0, \end{cases} \tag{1}$$

where y is an unknown function; f and ϕ are known analytic functions; α, τ , and the initial values λ_i are given; $[\alpha]$ is the smallest integer larger than or equal to α . In this paper, we introduce a new numerical method for solving fractional delay differential equations in Eq. (1). The method is based on the use of Taylor wavelets. We present the exact formula for determining the fractional integral of the Taylor wavelets. The exact formula will be then applied to solve the delay differential equation in Eq. (1). This formula allows us to reduce the given delay differential equation to a system of algebraic equations, which can be solved by the Newton iteration method.

The paper is organized as follows: Basic definitions and notations from Fractional Calculus are introduced in Sect. 2. Section 3 is devoted to Taylor wavelets and their properties. In Sect. 4, we establish the exact formula for determining the fractional integral of the Taylor wavelets defined in the previous section. A numerical method for solving the fractional delay differential equation based on Taylor wavelets is presented in Sect. 5 and error estimations are given in Sect. 6. Several examples are presented in Sect. 7 to show the applicability and the effectiveness of our method.

2 Fractional-order integrals and derivatives

In this section, we recall some definitions and basis properties of fractional-order integrals and derivatives.

Definition 2.1 (see [30]) The Riemann–Liouville fractional integral of order $\alpha \geq 0$ of a function $f(x)$ over $[0, +\infty)$ is a function over $[0, +\infty)$ defined as

$$(I^\alpha f)(x) = \begin{cases} \frac{1}{\Gamma(\alpha)} \int_0^x \frac{f(s)}{(x-s)^{1-\alpha}} ds = \frac{1}{\Gamma(\alpha)} x^{\alpha-1} * f(x), & \text{if } \alpha > 0, \\ f(x), & \text{if } \alpha = 0, \end{cases} \tag{2}$$

where $x^{\alpha-1} * f(x)$ is the convolution product of $x^{\alpha-1}$ and $f(x)$.

Definition 2.2 (see [31]) The Caputo fractional derivative of order $\alpha \geq 0$ of a function $f(x)$ over $[0, +\infty)$ is a function over $[0, +\infty)$ defined as

$$(D^\alpha f)(x) = I^{n-\alpha} f^{(n)}(x),$$

where $n = [\alpha]$.

Fractional-order integrals and derivatives satisfy the following properties:

Proposition 2.3 For $\alpha \geq 0$, the following hold:

1. I^α and D^α are linear operators, i.e., $I^\alpha(\lambda f + \mu g) = \lambda I^\alpha f + \mu I^\alpha g$ and $D^\alpha(\lambda f + \mu g) = \lambda D^\alpha f + \mu D^\alpha g$ for every functions f, g and numbers λ, μ .
2. $D^\alpha I^\alpha f(x) = f(x)$.
3. $I^\alpha D^\alpha f(x) = f(x) - \sum_{j=0}^{[\alpha]} \frac{f^{(j)}(0)}{j!} x^j$.
4. $I^\alpha x^j = \frac{\Gamma(j+1)}{\Gamma(j+\alpha+1)} x^{j+\alpha}$ for $j > -1$.
5. $D^\alpha x^j = \frac{\Gamma(j+1)}{\Gamma(j-\alpha+1)} x^{j-\alpha}$ for $j > \alpha - 1$.

3 Taylor wavelets

3.1 Wavelets and Taylor wavelets

Wavelets are a family of functions constructed from dilation and translation of a single function called the mother wavelet. When the dilation parameter a and the translation parameter b vary continuously, we have the following family of continuous wavelets [23]:

$$\psi_{a,b}(t) = |a|^{-\frac{1}{2}} \psi\left(\frac{t-b}{a}\right), \quad a \neq 0, \quad a, b \in \mathbb{R}$$

If we restrict the parameters a and b to discrete values as $a = a_0^k$, and $b = nb_0 a_0^k$, where $a_0 > 1, b_0 > 0$, and n and k are positive integers, we obtain the family of discrete wavelets as:

$$\psi_{k,n}(t) = |a_0|^{\frac{k}{2}} \psi(a_0^k t - nb_0),$$

which form a wavelet basis for $L^2(\mathbb{R})$.

Definition 3.1 (See [32]) Let k be a positive integer. For each $n = 1, \dots, 2^{k-1}$ and $m \in \mathbb{N}$, the Taylor wavelet function, say $\psi_{n,m}$, is defined over $[0, 1)$ by

$$\psi_{n,m}(x) = \begin{cases} 2^{\frac{k-1}{2}} \cdot \tilde{T}_m(2^{k-1}x - n + 1), & \text{if } \frac{n-1}{2^{k-1}} \leq x < \frac{n}{2^{k-1}}, \\ 0, & \text{otherwise,} \end{cases}$$

where

$$\tilde{T}_m(x) = \sqrt{2m+1} \cdot x^m \tag{3}$$

is the normal Taylor polynomial of degree m .

The six Taylor wavelets corresponding to $k = 2$ with the order $m < 3$ are the following:

$$\begin{aligned} \psi_{1,0}(x) &= \begin{cases} \sqrt{2}, & \text{if } 0 \leq x < \frac{1}{2}, \\ 0, & \text{if } \frac{1}{2} \leq x < 1. \end{cases} \\ \psi_{2,0}(x) &= \begin{cases} 0, & \text{if } 0 \leq x < \frac{1}{2}, \\ \sqrt{2}, & \text{if } \frac{1}{2} \leq x < 1. \end{cases} \\ \psi_{1,1}(x) &= \begin{cases} 2\sqrt{6}x, & \text{if } 0 \leq x < \frac{1}{2}, \\ 0, & \text{if } \frac{1}{2} \leq x < 1. \end{cases} \\ \psi_{2,1}(x) &= \begin{cases} 0, & \text{if } 0 \leq x < \frac{1}{2}, \\ \sqrt{6}(2x-1), & \text{if } \frac{1}{2} \leq x < 1. \end{cases} \\ \psi_{1,2}(x) &= \begin{cases} 4\sqrt{10}x^2, & \text{if } 0 \leq x < \frac{1}{2}, \\ 0, & \text{if } \frac{1}{2} \leq x < 1. \end{cases} \\ \psi_{2,2}(x) &= \begin{cases} 0, & \text{if } 0 \leq x < \frac{1}{2}, \\ \sqrt{10}(2x-1)^2, & \text{if } \frac{1}{2} \leq x < 1. \end{cases} \end{aligned}$$

The following properties of the Taylor wavelets can be verified by a direct calculation:

Proposition 3.2 Let k, n_1, n_2, m_1 , and m_2 be positive integers such that $1 \leq n_1, n_2 \leq 2^{k-1}$. Then,

$$\int_0^1 \psi_{n_1, m_1}(x) \psi_{n_2, m_2}(x) dx = \begin{cases} \frac{\sqrt{(2m_1+1)(2m_2+1)}}{m_1+m_2+1}, & \text{if } n_1 = n_2, \\ 0, & \text{if } n_1 \neq n_2. \end{cases}$$

3.2 Function approximation

Recall that a set $S \subset L^2[0, 1]$ is called a complete set if the linear vector space generated by S is dense in $L^2[0, 1]$. For each $k \in \mathbb{N}$, since the space of polynomials is dense in $L^2[0, 1]$, the set

$$\mathcal{O}_k := \bigcup_{m=0}^{\infty} \{\psi_{n,m}(x) \mid n = 1, \dots, 2^{k-1}\}$$

forms a complete set. Therefore, a function f in $L^2[0, 1]$ can always be expanded as

$$f(x) = \sum_{m=0}^{\infty} \sum_{n=1}^{2^{k-1}} c_{n,m} \psi_{n,m}(x), \tag{4}$$

for some sequence of real numbers $\{c_{n,m}\}_{n,m}$.

For each positive numbers k and M , we set

$$\mathcal{O}_{k,M} := \{\psi_{n,m}(x) \mid 1 \leq n \leq 2^{k-1}, 0 \leq m \leq M-1\}.$$

In the next section, we find a function in the linear vector space $\text{span}(\mathcal{O}_{k,M})$ which is the best approximation to a solution of a given fractional delay differential equation. The space $\text{span}(\mathcal{O}_{k,M})$ is a closed finite-dimensional subspace of $L^2[0, 1]$. By the Hilbert Projection Theorem (see [33, Thm. 2, p. 51]), there exists a unique function in $\text{span}(\mathcal{O}_{k,M})$ minimizing the distance to f . The function is obtained by truncating the series in Eq. (4) up to order $M-1$, i.e.,

$$f(x) \simeq \sum_{m=0}^{M-1} \sum_{n=1}^{2^{k-1}} c_{n,m} \psi_{n,m}(x) = C^T \cdot \Psi_{k,M}(x),$$

where

$$C = [c_{1,0}, \dots, c_{1,M-1}, c_{2,0}, \dots, c_{2,M-1}, \dots, c_{2^{k-1},0}, \dots, c_{2^{k-1},M-1}]^T, \tag{5}$$

and

$$\Psi_{k,M} = [\psi_{1,0}, \dots, \psi_{1,M-1}, \psi_{2,0}, \dots, \psi_{2,M-1}, \dots, \psi_{2^{k-1},0}, \dots, \psi_{2^{k-1},M-1}]^T. \tag{6}$$

4 Riemann–Liouville fractional integral for Taylor wavelets

An exact formula for the fractional-order integral of Taylor wavelets is presented in the following theorem:

Theorem 4.1 The integral of order $\alpha > 0$ of the function $\psi_{n,m}$ is given by

$$I^\alpha \psi_{n,m}(x) = \begin{cases} 0, & \text{if } 0 \leq x < \frac{(n-1)h}{2^{k-1}}, \\ U(x), & \text{if } \frac{(n-1)h}{2^{k-1}} \leq x < \frac{nh}{2^{k-1}}, \\ (x) - V(x), & \text{if } \frac{nh}{2^{k-1}} \leq x < 1, \end{cases} \quad (7)$$

where

$$U(x) = \frac{2^{(m+\frac{1}{2})(k-1)} \Gamma(m+1) \sqrt{2m+1}}{\Gamma(m+\alpha+1)} \cdot \left(x - \frac{(n-1)h}{2^{k-1}}\right)^{m+\alpha},$$

and

$$V(x) = \sum_{l=0}^m \binom{m}{l} \frac{2^{(l+\frac{1}{2})(k-1)} \Gamma(l+1) \sqrt{2m+1}}{\Gamma(l+\alpha+1)} \cdot \left(x - \frac{nh}{2^{k-1}}\right)^{l+\alpha}.$$

Proof To obtain $I^\alpha \psi_{n,m}$, we use the Laplace transform. Using the unit step function defined as

$$\mu_c(x) = \begin{cases} 1, & \text{if } x \geq c, \\ 0, & \text{if } x < c, \end{cases}$$

we can rewrite the Taylor wavelet $\psi_{n,m}(x)$ as follows:

$$\begin{aligned} \psi_{n,m}(x) &= \mu_{\frac{(n-1)h}{2^{k-1}}}(x) \cdot 2^{\frac{k-1}{2}} \tilde{T}_m(2^{k-1}x - n + 1) \\ &\quad - \mu_{\frac{nh}{2^{k-1}}}(x) \cdot 2^{\frac{k-1}{2}} \tilde{T}_m(2^{k-1}x - n + 1) \\ &= I_1 - I_2. \end{aligned}$$

By taking the Laplace transform of I_1 and using

$$\mathcal{L}\{\mu_c(x)f(x)\} = e^{-cs} \mathcal{L}\{f(x+c)\},$$

we get

$$\begin{aligned} \mathcal{L}\{I_1\} &= e^{-\frac{(n-1)h}{2^{k-1}}s} 2^{\frac{k-1}{2}} \mathcal{L}\left\{\tilde{T}_m\left(2^{k-1}\left(x + \frac{(n-1)h}{2^{k-1}}\right) - n + 1\right)\right\} \\ &= e^{-\frac{(n-1)h}{2^{k-1}}s} 2^{\frac{k-1}{2}} \mathcal{L}\{\tilde{T}_m(2^{k-1}x)\}. \end{aligned}$$

By substituting Eq. (3) to the right-hand side of the above equation, we obtain

$$\mathcal{L}\{I_1\} = e^{-\frac{(n-1)h}{2^{k-1}}s} 2^{\frac{k-1}{2}} \sqrt{2m+1} \mathcal{L}\{2^{m(k-1)}x^m\}.$$

Since $\mathcal{L}\{x^m\} = \frac{\Gamma(m+1)}{s^{m+1}}$, we have

$$\mathcal{L}\{I_1\} = 2^{(m+\frac{1}{2})(k-1)} \Gamma(m+1) \sqrt{2m+1} \cdot \frac{e^{-\frac{(n-1)h}{2^{k-1}}s}}{s^{m+1}}.$$

Similarly, we also have

$$\mathcal{L}\{I_2\} = \sum_{l=0}^m \binom{m}{l} 2^{(l+\frac{1}{2})(k-1)} \Gamma(l+1) \sqrt{2m+1} \cdot \frac{e^{-\frac{nh}{2^{k-1}}s}}{s^{l+1}}.$$

Using Eq. (2), we have

$$I^\alpha \psi_{n,m}(x) = \frac{1}{\Gamma(\alpha)} x^{\alpha-1} * \psi_{n,m}(x).$$

It is well-known that $\mathcal{L}\{f(x) * g(x)\} = \mathcal{L}\{f(x)\} \cdot \mathcal{L}\{g(x)\}$. Therefore,

$$\begin{aligned} \mathcal{L}\{I^\alpha \psi_{n,m}(x)\} &= \frac{1}{s^\alpha} \cdot \mathcal{L}\{\psi_{n,m}(x)\} \\ &= \frac{1}{s^\alpha} \cdot \mathcal{L}\{I_1\} - \frac{1}{s^\alpha} \cdot \mathcal{L}\{I_2\} \\ &= 2^{(m+\frac{1}{2})(k-1)} \Gamma(m+1) \sqrt{2m+1} \cdot \frac{e^{-\frac{(n-1)h}{2^{k-1}}s}}{s^{m+\alpha+1}} \\ &\quad - \sum_{l=0}^m \binom{m}{l} 2^{(l+\frac{1}{2})(k-1)} \Gamma(l+1) \sqrt{2m+1} \cdot \frac{e^{-\frac{nh}{2^{k-1}}s}}{s^{l+\alpha+1}}. \end{aligned}$$

By taking the inverse Laplace transformation, we get

$$\begin{aligned} I^\alpha \psi_{n,m}(x) &= \frac{2^{(m+\frac{1}{2})(k-1)} \Gamma(m+1) \sqrt{2m+1}}{\Gamma(m+\alpha+1)} \\ &\quad \cdot \left(x - \frac{(n-1)h}{2^{k-1}}\right)^{m+\alpha} \cdot \mu_{\frac{(n-1)h}{2^{k-1}}}(x) \\ &\quad - \sum_{l=0}^m \binom{m}{l} \frac{2^{(l+\frac{1}{2})(k-1)} \Gamma(l+1) \sqrt{2m+1}}{\Gamma(l+\alpha+1)} \\ &\quad \cdot \left(x - \frac{nh}{2^{k-1}}\right)^{l+\alpha} \cdot \mu_{\frac{nh}{2^{k-1}}}(x) \end{aligned}$$

The theorem then follows. □

5 Numerical solutions of fractional delay differential equations

In this section, we present a new numerical method for solving the fractional delay differential equation given in Eq. (1).

We fix a positive integer k . The function $D^\alpha y(x)$ can be expanded over $[0, 1)$ as

$$D^\alpha y(x) \simeq \sum_{m=0}^{M-1} \sum_{n=1}^{2^{k-1}} c_{n,m} \psi_{n,m}(x) = C^T \Psi_{k,M}(x), \tag{8}$$

where C and $\Psi_{k,M}$ are given in Eqs. (5) and (6), respectively. By applying the integral operator I^α to both sides of Eq. (8) and using item 3 in Proposition 2.3 with $y^{(j)}(0) = \lambda_j$ for $j = 0, \dots, [\alpha]$, we obtain

$$y(x) \simeq \begin{cases} C^T I^\alpha \Psi_{k,M}(x) + \sum_{j=0}^{[\alpha]} \frac{\lambda_j}{j!} x^j, & \text{if } x \in [0, 1), \\ \phi(x), & \text{if } x < 0. \end{cases} \tag{9}$$

Therefore,

$$y(x - \tau) \simeq \begin{cases} C^T I^\alpha \Psi_{k,M}(x - \tau) + \sum_{j=0}^{[\alpha]} \frac{\lambda_j}{j!} (x - \tau)^j, & \text{if } x \in [\tau, 1), \\ \phi(x - \tau), & \text{if } x < \tau. \end{cases} \tag{10}$$

By substituting Eqs. (8), (9) and (10) to the given fractional delay differential equation in Eq. (1) and using Eq. (7), we obtain an algebraic equation. We collocate this algebraic equation at the following $2^{k-1}M$ Newton–Cotes nodes

$$x_i = \frac{2i - 1}{2^k M}, \quad i = 1, \dots, 2^{k-1}M,$$

we then obtain a system of $2^{k-1}M$ algebraic equations in the $2^{k-1}M$ unknown constants $c_{n,m}$. The last system can be solved using Newton’s iteration method. The initial guess for Newton’s iterative method can be obtained similarly to the method given in [34] as follows. To choose the initial guesses, in the first stage, we set $k = 1$ and $M = 1$ and then apply Newton’s iterative method for solving the given system of equations. In this stage, we obtain an approximation to our problem. Next, we increase the value of M until a satisfactory convergence is achieved. We then set $k = 2$ and use the approximate solution in the first stage as our initial guess in this stage. We continue this approach until the results are similar up to a required number of decimal places for the same k and two consecutive M values.

6 Error estimation

In this section, we estimate the error bound for the best approximation based on Taylor wavelets.

Theorem 6.1 Let $f \in L^2[0, 1]$ such that f is M times differentiable. Let $C^T \Psi_{k,M}$ be the best approximation of f in $\mathcal{O}_{k,M}$. Then,

$$\|f - C^T \Psi_{k,M}\|_2 \leq \frac{2N}{M! 2^{M(k+1)}}, \tag{11}$$

where $N = \max_{\xi \in [0,1]} |f^{(M)}(\xi)|$.

Proof We divide the closed interval $[0, 1]$ into 2^{k-1} subintervals $I_n = \left[\frac{n-1}{2^{k-1}}, \frac{n}{2^{k-1}}\right]$ with $n = 1, \dots, 2^{k-1}$. By the definition of Taylor wavelets, for every $n = 1, \dots, 2^{k-1}$, the function $C^T \Psi_{k,M}$ is also the best approximation of f over the interval I_n . We denote $P_{n,M-1}(x)$ to be the interpolating polynomial of f at the Chebyshev nodes in the interval I_n . Due to [35, Chp. 20], the interpolation error is

$$\begin{aligned} |f(x) - P_{n,M-1}(x)| &\leq \frac{1}{2^{M-1}M!} \left(\frac{|I_n|}{2}\right)^M \cdot \max_{\xi \in I_n} |f^{(M)}(\xi)| \\ &\leq \frac{2N}{2^{M(k+1)}M!}. \end{aligned}$$

Let P_{M-1} be the function defined over $[0, 1)$ such that $P_{M-1}(x) = P_{n,M-1}(x)$ for every $x \in \left[\frac{n-1}{2^{k-1}}, \frac{n}{2^{k-1}}\right)$, $n = 1, \dots, 2^{k-1}$. Then,

$$|f(x) - P_{M-1}(x)| \leq \frac{2N}{2^{M(k+1)}M!}, \quad \text{for every } x \in [0, 1). \tag{12}$$

Since $C^T \Psi_{k,M}$ is the best approximation of f in $\mathcal{O}_{k,M}$ and that $P_{M-1} \in \mathcal{O}_{k,M}$, we conclude from Eq. (12) that

$$\begin{aligned} \|f - C^T \Psi_{k,M}\|_2^2 &\leq \|f - P_{M-1}\|_2^2 \\ &= \int_0^1 (f(x) - P_{M-1}(x))^2 dx \\ &\leq \int_0^1 \left(\frac{2N}{2^{M(k+1)}M!}\right)^2 dx = \left(\frac{2N}{2^{M(k+1)}M!}\right)^2. \end{aligned}$$

□

Theorem 6.2 Let $f \in L^2[0, 1]$ such that f is M times differentiable. Let $C^T\Psi_{k,M}$ be the best approximation of f in $\mathcal{O}_{k,M}$. Then,

$$\|I^\alpha f - I^\alpha C^T\Psi_{k,M}\|_2 \leq \frac{2N}{\Gamma(\alpha)\sqrt{2\alpha(2\alpha - 1)}2^{M(k+1)}M!},$$

where $N = \max_{\xi \in [0,1]} |f^{(M)}(\xi)|$.

Proof Using Eq. (2) and Hölder’s inequality, we can estimate the difference between $I^\alpha f$ and $I^\alpha C^T\Psi$ at $x \in [0, 1]$ as follows:

$$\begin{aligned} &|I^\alpha f(x) - I^\alpha C^T\Psi_{k,M}(x)| \\ &\leq \frac{1}{\Gamma(\alpha)} \int_0^x \frac{|f(s) - C^T\Psi_{k,M}(s)|}{(x-s)^{1-\alpha}} ds \\ &\leq \frac{1}{\Gamma(\alpha)} \left(\int_0^x \frac{ds}{(x-s)^{2-2\alpha}} \right)^{\frac{1}{2}} \left(\int_0^x (f(s) - C^T\Psi(s))^2 ds \right)^{\frac{1}{2}} \\ &\leq \frac{x^{\alpha-\frac{1}{2}}}{\Gamma(\alpha)\sqrt{2\alpha-1}} \|f - C^T\Psi_{k,M}\|_2. \end{aligned}$$

Finally, we apply Eq. (11) and obtain

$$\begin{aligned} &\|I^\alpha f - I^\alpha C^T\Psi_{k,M}\|_2 \\ &\leq \frac{1}{\Gamma(\alpha)\sqrt{2\alpha-1}} \|x^{\alpha-\frac{1}{2}}\|_2 \cdot \|f - C^T\Psi_{k,M}\|_2 \\ &= \frac{2N}{\Gamma(\alpha)\sqrt{2\alpha(2\alpha - 1)}2^{M(k+1)}M!}. \end{aligned}$$

7 Illustrative examples

In this section, we compare the efficiency of our method with that of some previously known ones.

Example 7.1 Consider the following fractional delay differential equation (see [21, Example 1]):

$$\begin{aligned} D^\alpha y(x) = &y(x - \tau) - y(x) + \frac{2x^{2-\alpha}}{\Gamma(3 - \alpha)} - \frac{x^{1-\alpha}}{\Gamma(2 - \alpha)} \\ &+ 2\tau x - \tau^2 - \tau, \end{aligned} \tag{13}$$

where $x \in [0, 1]$, $\alpha \in (0, 1]$ and $y(x) = x^2 - x$ if $x \leq 0$.

We choose $k = 2$ and $M = 3$ and approximate $D^\alpha y(x)$ as

$$\begin{aligned} D^\alpha y(x) \simeq &c_{1,0}\psi_{1,0}(x) + c_{1,1}\psi_{1,1}(x) + c_{1,2}\psi_{1,2}(x) \\ &+ c_{2,0}\psi_{2,0}(x) + c_{2,1}\psi_{2,1}(x) + c_{2,2}\psi_{2,2}(x) \\ = &C^T \cdot \Psi_{2,2}(x), \end{aligned}$$

where $C = [c_{1,0}, c_{1,1}, c_{1,2}, c_{2,0}, c_{2,1}, c_{2,2}]^T$ is the vector of unknown constants that we need to determine. Then, we have

$$y(x) = \begin{cases} C^T I^\alpha \Psi_{2,2}(x), & \text{if } x \in [0, 1], \\ x^2 - x, & \text{if } x \leq 0, \end{cases} \tag{14}$$

and

$$y(x - \tau) = \begin{cases} C^T I^\alpha \Psi_{2,2}(x - \tau), & \text{if } x \in [\tau, \tau + 1], \\ (x - \tau)^2 - x + \tau, & \text{if } x \leq \tau. \end{cases} \tag{15}$$

In the above formulas, $I^\alpha \Psi_{2,2}$ are determined explicitly by Theorem 4.1. By substituting Eqs. (14) and (15) to Eq. (13), we obtain an algebraic equation. By collocating the algebraic equation at Newton–Cotes nodes

$$x_i = \frac{2i - 1}{12}, \quad i = 1, \dots, 6,$$

we get a linear system in the $c_{n,m}$ ’s.

In case there is no delay, i.e. $\tau = 0$, the linear system becomes

$$\square \begin{cases} 36\sqrt{2}c_{1,0} + 6\sqrt{6}c_{1,1} + \sqrt{10}c_{1,2} = -30, \\ 4\sqrt{2}c_{1,0} + 2\sqrt{6}c_{1,1} + \sqrt{10}c_{1,2} = -2, \\ 36\sqrt{2}c_{1,0} + 30\sqrt{6}c_{1,1} + 25\sqrt{10}c_{1,2} = -6, \\ 36\sqrt{2}c_{2,0} + 6\sqrt{6}c_{2,1} + \sqrt{10}c_{2,2} = 6, \\ 4\sqrt{2}c_{2,0} + 2\sqrt{6}c_{2,1} + \sqrt{10}c_{2,2} = 2, \\ 36\sqrt{2}c_{2,0} + 30\sqrt{6}c_{2,1} + 25\sqrt{10}c_{2,2} = 30. \end{cases}$$

This system admits the unique solution:

$$\begin{aligned} c_{1,0} = &-\frac{1}{\sqrt{2}}, \quad c_{1,1} = \frac{1}{\sqrt{6}}, \quad c_{1,2} = 0, \\ c_{2,0} = &0, \quad c_{2,1} = \frac{1}{\sqrt{6}}, \quad c_{2,2} = 0. \end{aligned}$$

By substituting this solution to Eq. (14), we obtain $y(x) = x^2 - x$, which is the exact solution of the given delay

differential equation. It is noted that the exact solution was not obtained in [21].

In case there is delay, we obtain approximations of the solutions depending on α and τ . In Table 1, we demonstrate the absolute errors for our method by selecting $k = 2$ and $M = 3$ or with the number of bases $\hat{m} = 2^{k-1}M = 6$; by the Bernoulli wavelet method in [21] by selecting $k = 2$ and $M_1 = 3$ or with the same number of bases. The values in Table 1 suggest that numerical solutions produced from our method have less absolute errors than numerical solutions from the Bernoulli wavelet method in [21]. In Table 1, M_1 is the degree of Bernoulli polynomials. Figure 1 shows the graphs of the exact solution and our approximate solution when $\alpha = 1$ and the delay $\tau = 0.01$.

Example 7.2 Consider the following fractional-order delay differential equation (see [21, Example 2]):

$$\begin{cases} D^\alpha y(x) = -y(x) - y(x - 0.3) + e^{-x+0.3}, & x \in [0, 1], \alpha \in (2, 3], \\ y(0) = 1, y'(0) = -1, y''(0) = 1, \\ y(x) = e^{-x}, & x < 0. \end{cases}$$

This problem admits the exact solution $y(x) = e^{-x}$ when $\alpha = 3$. In Table 2, we show some values of the exact

solution and the numerical solutions obtained by applying our method by choosing $k = 2, M = 7$ or with the number of bases $\hat{m} = 14$; by Bernoulli wavelet method in [21] by selecting $k = 2, M_1 = 7$ or with the same number of bases; by Hermit wavelet method in [36] by selecting $k = 1, M_2 = 25$ or with the number of bases $\hat{m} = 2^{k-1}M_2 = 25$. In this table, M_2 is the degree of the Hermit polynomials. Figure 2 represents the graph of the absolute error function of the numerical solution obtained from our method when $\alpha = 3, k = 2$, and $M = 7$. In addition, Fig. 3 shows the graphs of the exact solution and the numerical solutions for different order α . The graphical detail of Fig. 3 suggests that the numerical solutions approach the exact solution when the order α tends to 3.

Example 7.3 Consider the following fractional-order delay differential equation (see [37, Example 6]):

$$\begin{cases} D^\alpha y(x) = y(x - 1) + u(x), & x \in (0, 2], \\ y(x) = 1, & x \leq 0, \end{cases} \tag{16}$$

where $\alpha \in (0, 1]$ and the function $u(x)$ is defined by

$$u(x) = \begin{cases} -2.1 + 1.05x, & x \in (0, 1], \\ -1.05, & x \in (1, 2]. \end{cases}$$

Table 1 The absolute errors for numerical solutions of Example 7.1 when $\alpha = 1$ from our method and the Bernoulli wavelet method in [21]

x	Our method with $k = 2$ and $M = 3$			Method in [21] with $k = 2$ and $M_1 = 3$		
	$\tau = 0.0001$	$\tau = 0.001$	$\tau = 0.01$	$\tau = 0.0001$	$\tau = 0.001$	$\tau = 0.01$
0.2	0	8.33×10^{-17}	2.78×10^{-17}	8.33×10^{-17}	1.94×10^{-16}	0
0.4	5.55×10^{-17}	1.11×10^{-16}	5.55×10^{-17}	2.22×10^{-16}	3.33×10^{-16}	1.11×10^{-16}
0.6	1.67×10^{-16}	1.11×10^{-16}	1.11×10^{-16}	1.47×10^{-14}	8.60×10^{-14}	3.15×10^{-14}
0.8	1.11×10^{-16}	2.22×10^{-16}	2.22×10^{-16}	1.57×10^{-14}	8.57×10^{-14}	3.23×10^{-14}

Fig. 1 The left-hand side is the graph of the exact solution (line) and the approximation solution (dashed) for Example 7.1 from our method when $k = 2, M = 3, \alpha = 1$, and $\tau = 0.01$. The right-hand side is the graph of the absolute error function

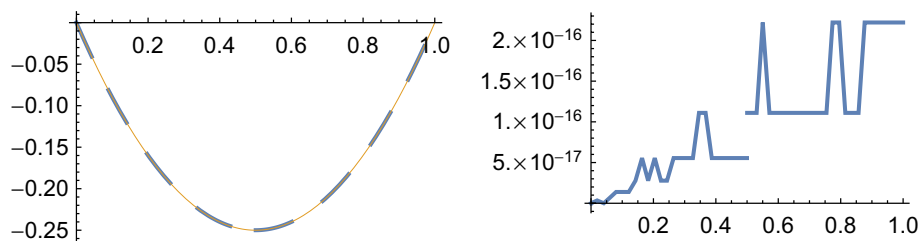


Table 2 The exact solution for Example 7.2 with $\alpha = 3$ and numerical solutions obtained from our method, Hermit wavelet method in [36], and Bernoulli wavelet method in [21]

x	Exact solution	Hermit wavelets [36] $k = 1, M_2 = 25$	Bernoulli wavelets [21] $k = 2, M_1 = 7$	Present method $k = 2, M = 7$
0.0	1	1	1	1
0.2	0.8187307531	0.8187	0.8187	0.8187307531
0.4	0.6703200460	0.6703	0.6703	0.6703200460
0.6	0.5488116361	0.5488	0.5488	0.5488116361
0.8	0.4493289641	0.4493	0.4494	0.4493289641

Fig. 2 The left-hand side is the graph of the exact solution (line) and the numerical solution (dashed) for Example 7.2 from our method. The right-hand side is the graph of the absolute error function. Here, we choose $k = 2$, $M = 7$, and $\alpha = 3$

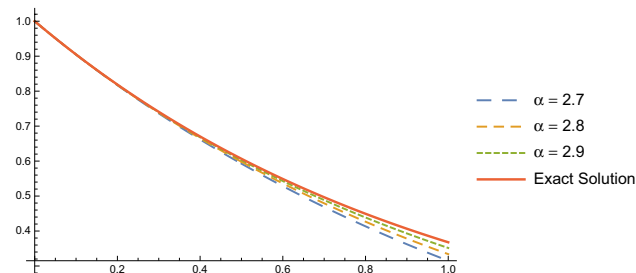
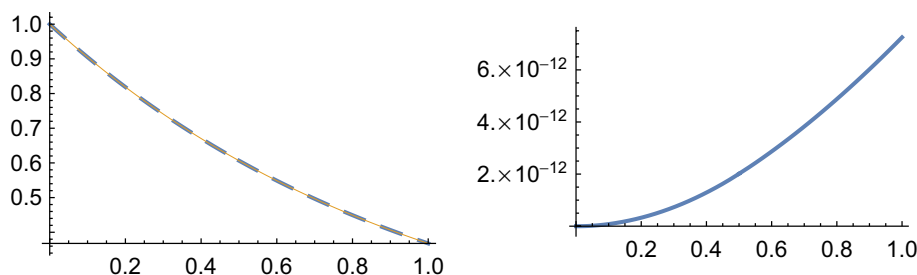


Fig. 3 The graphs of the exact solutions and the numerical solutions for Example 7.2 when $k = 2$, $M = 4$, and $\alpha = 2.7, 2.8, 2.9$

In case $\alpha = 1$, this problem admits the exact solution

$$y(x) = \begin{cases} 1 - 1.1x + 0.525x^2, & x \in (0, 1], \\ -0.25 + 1.575x - 1.075x^2 + 0.175x^3, & x \in (1, 2]. \end{cases}$$

To apply our method, we make a transformation of unknown functions $g(x) = y(2x)$, and set $t = \frac{x}{2}$ with $t \in (0, 1]$. We then have

$$y(x) = g\left(\frac{x}{2}\right) = g(t), \tag{17}$$

$$y(x - 1) = g\left(\frac{x-1}{2}\right) = g\left(t - \frac{1}{2}\right), \tag{18}$$

and

$$D^\alpha y(x) = 2^{-\alpha} D^\alpha g\left(\frac{x}{2}\right) = 2^{-\alpha} D^\alpha g(t). \tag{19}$$

By substituting Eqs. (17)–(19) to (16), the given differential equation is transformed to the following equivalent one:

$$\begin{cases} 2^{-\alpha} D^\alpha g(t) = g\left(t - \frac{1}{2}\right) + u(2t), & t \in (0, 1], \\ g(t) = 1, & t \leq 0, \end{cases}$$

where $\alpha \in (0, 1]$. In case $\alpha = 1$, by applying our method, we obtain the exact solution.

Table 3 The residue errors for numerical solutions of Example 7.3 from our method and the Legendre multiwavelet collocation method in [37] when $\alpha = 0.95$

t	Our method with $k = 2$		Method in [37] with $k = 2$	
	$M = 7$	$M = 10$	$M_3 = 7$	$M_3 = 10$
0.2	1.77×10^{-15}	1.11×10^{-14}	1.92×10^{-4}	$1.49 \cdot 10^{-5}$
0.4	9.77×10^{-15}	2.76×10^{-13}	1.36×10^{-5}	$1.61 \cdot 10^{-6}$
0.6	2.73×10^{-14}	2.89×10^{-12}	9.72×10^{-6}	$1.13 \cdot 10^{-6}$
0.8	4.13×10^{-14}	1.83×10^{-11}	6.10×10^{-5}	$4.47 \cdot 10^{-6}$
1.2	8.31×10^{-6}	2.50×10^{-6}	3.11×10^{-5}	$1.56 \cdot 10^{-6}$
1.4	4.00×10^{-6}	2.57×10^{-7}	2.85×10^{-6}	$2.17 \cdot 10^{-7}$
1.6	2.90×10^{-6}	0.81×10^{-7}	2.40×10^{-6}	$1.81 \cdot 10^{-7}$
1.8	2.88×10^{-6}	7.79×10^{-7}	1.72×10^{-5}	$8.23 \cdot 10^{-7}$

In case $\alpha \neq 1$, the exact solution is not known. In this case, to show the efficiency of the present method, we consider the residual error

$$D^\alpha y(x) - y(x - 1) - u(x) = 2^{-\alpha} D^\alpha g(t) - g\left(t - \frac{1}{2}\right) - u(2t).$$

In Table 3, we compare the residual errors of numerical solutions obtained from our method and Legendre multiwavelet collocation method in [37] with $\alpha = 0.95$. For computing the numerical solution by applying our method, we select $k = 2$ with $M = 7$ or with the number of bases $\hat{m} = 14$ and by selecting $k = 2$ with $M = 10$ or with the number of bases $\hat{m} = 20$; together with the Legendre multiwavelet collocation method in [37] using $k = 2$ with $M_3 = 7$ and $k = 2$ with $M_3 = 10$ (hence with the same number of bases). In this table, M_3 stand for the degrees of the Legendre wavelets. The left-hand side of Fig. 4 demonstrates the graph of the exact solution with $\alpha = 1$ and the numerical solution from our method with $k = 2$ and $M = 3$, while the right-hand side is the graph of the absolute error function. Figure 5 represents the graphs of different numerical solutions with different values of α with $k = 2$ and $M = 3$. From Fig. 5, we see that as α approaches to 1, the numerical solutions approach to the exact solution of the given differential equation with the integer order.

Fig. 4 The graphs on the left-hand side are of the numerical solution for Example 7.3 obtained from our computation (dashed) and the exact solution when $k = 2$ and $M = 3$. The graph of the absolute error is showed on the right-hand side

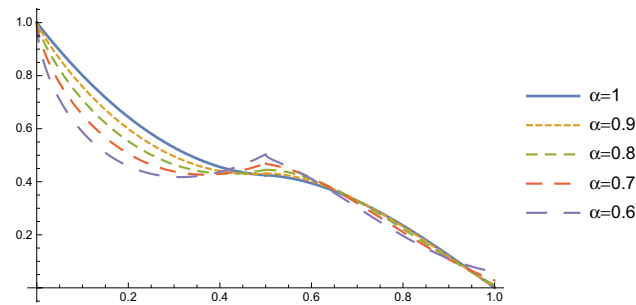
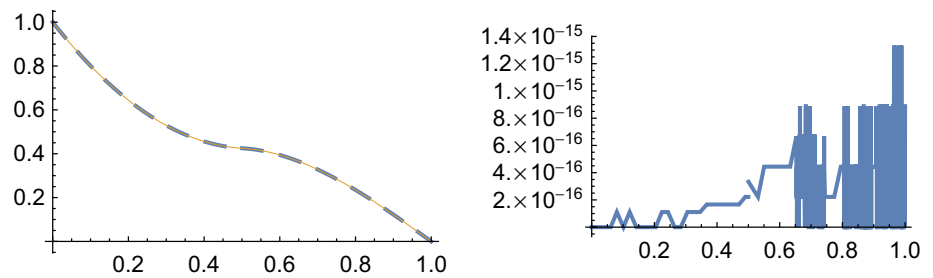


Fig. 5 The graphs of the numerical solutions for Example 7.3 obtained from our computation for $k = 2$ and $M = 3$ and different values of α

8 Conclusion

In this paper, we propose an exact formula for the Riemann–Liouville fractional integral of a Taylor wavelet. A new numerical method for delay fractional differential equations is presented. Using the exact formula and collocation method, we reduce the problem of computing a numerical solution of a delay fractional differential equation to the problem of solving an algebraic system. Several examples are demonstrated to show the applicability and the efficiency of the present method.

Acknowledgements The authors wish to express their sincere thanks to anonymous referees for their valuable suggestions that improved the final manuscript.

References

- Oldham KB (2010) Fractional differential equations in electrochemistry. *Adv Eng Softw* 41(1):9–12
- Baillie RT (1996) Long memory processes and fractional integration in econometrics. *J Econom* 73(1):5–59
- Carpinteri A, Mainardi F (eds) (2014) *Fractals and fractional calculus in continuum mechanics*. Springer, Berlin
- Rossikhin YA, Shitikova MV (1997) Applications of fractional calculus to dynamic problems of linear and nonlinear hereditary mechanics of solids. *Appl Mech Rev* 50(1):15–67
- Hall MG, Barrick TR (2008) From diffusion-weighted MRI to anomalous diffusion imaging. *Magn Reson Med* 59(3):447–455
- Povstenko Y (2010) Signaling problem for time-fractional diffusion-wave equation in a half-space in the case of angular symmetry. *Nonlinear Dyn* 59(4):593–605
- He JH (1999) Some applications of nonlinear fractional differential equations and their approximations. *Bull Sci Technol* 15(2):86–90
- Mandelbrot B (1967) Some noises with 1/f spectrum, a bridge between direct current and white noise. *IEEE Trans Inf Theory* 13(2):289–298
- Ockendon JR, Tayler AB (1971) The dynamics of a current collection system for an electric locomotive. *Proc R Soc Lond A Math Phys Sci* 322(1551):447–468
- Aiello WG, Freedman HI, Wu J (1992) Analysis of a model representing stage-structured population growth with state-dependent time delay. *SIAM J Appl Math* 52(3):855–869
- Evans DJ, Raslan KR (2005) The Adomian decomposition method for solving delay differential equation. *Int J Comput Math* 82(1):49–54
- Wang WS, Li SF (2007) On the one-leg θ -methods for solving nonlinear neutral functional differential equations. *Appl Math Comput* 193(1):285–301
- Yu ZH (2008) Variational iteration method for solving the multi-pantograph delay equation. *Phys Lett A* 372(43):6475–6479
- Hafshejani MS, Vanani SK, Hafshejani JS (2011) Numerical solution of delay differential equations using Legendre wavelet method. *World Appl Sci J* 13:27–33
- Sedaghat S, Ordokhani Y, Dehghan M (2012) Numerical solution of the delay differential equations of pantograph type via Chebyshev polynomials. *Commun Nonlinear Sci Numer Simul* 17(12):4815–4830
- Tohidi E, Bhrawy AH, Erfani K (2013) A collocation method based on Bernoulli operational matrix for numerical solution of generalized pantograph equation. *Appl Math Model* 37(6):4283–4294
- Moghaddam BP, Mostaghim ZS (2013) A numerical method based on finite difference for solving fractional delay differential equations. *J Taibah Univ Sci* 7(3):120–127
- Khader MM, Hendy AS (2012) The approximate and exact solutions of the fractional-order delay differential equations using Legendre pseudospectral method. *Int J Pure Appl Math* 74(3):287–297
- Yang Y, Huang Y (2013) Spectral-collocation methods for fractional pantograph delay-integro-differential equations. *Adv Math Phys*
- Saeed U (2014) Hermite wavelet method for fractional delay differential equations. *J Differ Equ Appl*
- Rahimkhani P, Ordokhani Y, Babolian E (2017) A new operational matrix based on Bernoulli wavelets for solving fractional delay differential equations. *Numer Algorithms* 74(1):223–245
- Wang Z (2013) A numerical method for delayed fractional-order differential equations. *J Appl Math*
- Razzaghi M, Yousefi S (2001) The Legendre wavelets operational matrix of integration. *Int J Syst Sci* 32(4):495–502

24. Beylkin G, Coifman R, Rokhlin V (1991) Fast wavelet transforms and numerical algorithms I. *Commun Pure Appl Math* 44(2):141–183
25. Zhu L, Fan Q (2012) Solving fractional nonlinear Fredholm integro-differential equations by the second kind Chebyshev wavelet. *Commun Nonlinear Sci Numer Simul* 17(6):2333–2341
26. Heydari MH, Hooshmandasl MR, Mohammadi F (2014) Legendre wavelets method for solving fractional partial differential equations with Dirichlet boundary conditions. *Appl Math Comput* 234:267–276
27. Saeedi H, Moghadam MM, Mollahasani N, Chuev GN (2011) A CAS wavelet method for solving nonlinear Fredholm integro-differential equations of fractional order. *Commun Nonlinear Sci Numer Simul* 16(3):1154–1163
28. Li Y, Zhao W (2010) Haar wavelet operational matrix of fractional order integration and its applications in solving the fractional order differential equations. *Appl Math Comput* 216(8):2276–2285
29. Keshavarz E, Ordokhani Y, Razzaghi M (2014) Bernoulli wavelet operational matrix of fractional order integration and its applications in solving the fractional order differential equations. *Appl Math Model* 38(24):6038–6051
30. Miller KS, Ross B (1993) *An introduction to the fractional calculus and fractional differential equations*. Wiley, New York
31. Caputo M (1967) Linear models of dissipation whose Q is almost frequency independent-II. *Geophys J Int* 13(5):529–539
32. Keshavarz E, Ordokhani Y, Razzaghi M (2018) The Taylor wavelets method for solving the initial and boundary value problems of Bratu-type equations. *Appl Numer Math* 128:205–216
33. Luenberger DG (1997) *Optimization by vector space methods*. Wiley, Hoboken
34. Yuttanan B, Razzaghi M (2019) Legendre wavelets approach for numerical solutions of distributed order fractional differential equations. *Appl Math Model* 70:350–364
35. Stewart GW (1993) *Afternotes on numerical analysis*. University of Maryland at College Park
36. Saeed U, Rehman M (2014) Hermite wavelet method for fractional delay differential equations. *J Differ Equ Appl*
37. Yousefi S, Lotfi A (2013) Legendre multiwavelet collocation method for solving the linear fractional time delay systems. *Cent Eur J Phys* 11(10):1463–1469

Publisher's Note Springer Nature remains neutral with regard to jurisdictional claims in published maps and institutional affiliations.